

N O T I C E

THIS DOCUMENT HAS BEEN REPRODUCED FROM
MICROFICHE. ALTHOUGH IT IS RECOGNIZED THAT
CERTAIN PORTIONS ARE ILLEGIBLE, IT IS BEING RELEASED
IN THE INTEREST OF MAKING AVAILABLE AS MUCH
INFORMATION AS POSSIBLE

NASA Technical Memorandum 81582

OBSERVATION OF PRESSURE VARIATION IN THE CAVITATION REGION OF SUBMERGED JOURNAL BEARINGS

(NASA-TM-81582) OBSERVATION OF PRESSURE
VARIATION IN THE CAVITATION REGION OF
SUBMERGED JOURNAL BEARINGS (NASA) 27 p
HC A03/MF A01

N80-31798

CSSL 131

Unclass

G3/37

28731

I. Etsion and L. P. Ludwig
Lewis Research Center
Cleveland, Ohio

Prepared for the
Lubrication Conference sponsored by the
American Society of Mechanical Engineers
New Orleans, Louisiana, October 11-14, 1981



NASA

OBSERVATION OF PRESSURE VARIATION IN THE CAVITATION REGION
OF SUBMERGED JOURNAL BEARINGS

by I. Etsion and L. P. Ludwig

National Aeronautics and Space Administration
Lewis Research Center
Cleveland, Ohio 44135

L-555

Visual observations and pressure measurements in the cavitation zone of a submerged journal bearing are described. Tests were performed at various shaft speeds and ambient pressure levels. Some photographs of the cavitation region are presented showing strong reverse flow at the downstream end of the region. Pressure profiles are presented showing significant pressure variations inside the cavitation zone, contrary to common assumptions of constant cavitation pressure.

NOMENCLATURE

D	bearing diameter
L	bearing length
N	shaft speed, rpm
p	pressure
p_s	ambient supply pressure on both sides of bearing
T	inlet oil temperature
Z	axial position measured from mid-section of bearing
θ	angular position measured from maximum clearance in direction of shaft rotation
θ_0	angular position of minimum film pressure
θ_{end}	angular position of cavitation end
θ_{st}	angular position of cavitation start

INTRODUCTION

Cavitation has been recognized long ago as an important phenomenon in hydrodynamic lubrication. A great deal of work on cavitation in bearings has been published in the literature. However, most of the effort has been devoted to mathematical modeling of the conditions at the start of cavitation in converging-diverging lubricating films. A good review of the various existing models and hypotheses on cavitation is presented in Ref. [1]. Although in some aspects these various models differ from each other they all share a common assumption of a uniform pressure in the cavitation region. There is at the present an uncertainty regarding the exact value of the cavitation pressure. However, it is generally accepted that once the cavitation occurs this pressure remains constant all over the cavitation region and on its boundaries.

When a cavity of either the vapor or gaseous type, as defined in [1], is completely enclosed by the liquid lubricant, a mathematical modeling of the conditions at the downstream end of the cavitation region is also necessary. Enclosed cavitations are typical in submerged bearings, squeeze-film dampers, and seals. Representative theoretical analyses on cavitation in these machine elements can be found in Refs. [2], [3], and more recently, in [4], [5], and [6]. Again, all these analyses are based on the assumption of a constant pressure inside and on the boundaries of the cavitation region.

A shortcoming of the constant pressure assumption is pointed out in a discussion of Ref. [4] and in Ref. [5]. By using the short bearing solution of the Reynolds equation it can be shown that a constant cavity pressure results in pressure discontinuity at the downstream tip of the cavitation region. This is due to the fact that immediately at this tip the pressure resumes its full film value as if cavitation did not exist. In Ref. [5] it

is argued that this deficiency can be overcome by a singular perturbation analysis. However, even when the complete Reynolds equation is solved the circumferential pressure gradient at the downstream boundary of the cavitation is still very large as can be seen in Fig. 7 of Ref. [4]. Such a sharp increase in pressure over a very short distance seems unreasonable, making the constant pressure assumption somewhat questionable.

Considering the importance of cavitation in hydrodynamic lubrication, it is surprising that so little is known about the actual pressure in the cavitation region. Most of the experimental work on cavitation is limited to observing of the cavity extent through transparent walls of bearings and seals, e.g., [2] and [4]. The few pressure measurements are limited in scope, aiming toward the sub-cavity pressure loop immediately upstream of the cavitation region. Some of these experimental observations are also reviewed in Ref. [1].

The lack of more information on the cavitation pressure, and particularly of its behavior at the downstream end of enclosed cavitated regions inspired the present work. Its objectives were (1) to more closely observe the reformation region of enclosed cavitation, and (2) to extensively map the pressure inside the cavitation region.

APPARATUS AND PROCEDURE

Figure 1, which is a schematic of the test apparatus, depicts the journal bearing configuration that was used to study cavitation. Figures 2 and 3 are photographs of the test apparatus. A rotor 5.08 cm diameter and 3.81 cm long ($L/D = 0.75$) was mounted on a commercial grinding spindle which provided rotor O.D. runouts of less than 0.00127 cm. A variable speed drive allowed a speed test range from 1000 to 5000 rpm.

An acrylic plastic housing allowed visual observation of the cavitation region. This housing was mounted on a motor driven indexing fixture which permitted rotation of the housing through 360° . The indexing fixture, in turn was mounted on a linear slid which permitted axial translation of the housing. These two degrees of freedom of housing motion permitted scanning the entire cavitation region with a single pressure tap which is depicted in Fig. 1. A differential type pressure transducer was employed in order to detect any subatmospheric pressures which may be associated with cavitation. In general, the scanning procedure included rig operation at a constant speed and supply pressure until thermal equilibrium was established as indicated by "oil in" and "oil out" temperatures. After thermal equilibrium was obtained the indexing fixture was used to select the first scan position, this generally was in the full fluid film region upstream or downstream of the cavitation region. The housing was then moved axially, and the pressure recorded on a x-y plotter which provided a trace of pressure amplitude as a function of axial position. The next trace was taken by rotating the housing 5° and then moving in an axial direction. This was repeated in 5° increments until the entire cavitation region was scanned. The maximum clearance was defined to be at the angular position where the scan outside the cavitation region boundaries showed a constant axial pressure equal to the ambient pressure. This method could produce an inaccuracy of $\pm 5^\circ$ in the apparant location of the maximum clearance. Angular position was measured from the line of maximum clearance as defined above, and axial position was measured from the mid-plane of the bearing as shown in Fig. 4.

Eccentricity between the rotor and housing was established by use of shims to adjust the housing centerline with respect to the rotor centerline;

an eccentricity of 0.4 was used for all the data reported herein. Since the average radial clearance was 0.0114 cm, the minimum clearance due to the 0.4 eccentricity was 0.00684 cm.

Both ends of the bearing were flooded with oil; this was accomplished by use of "oil in" and "oil out" ports on both ends of the bearing. The "oil in" temperature was controlled by a heat exchanger and generally was between 30° to 38° C. Oil pressure at both ends of the bearings was the same and was varied between 13 and 55 KPa in order to determine the effect of supply pressure on cavitation. The maximum pressure of 55 KPa was determined by the capacity of the lip seal in the test apparatus.

Still and motion pictures were taken of the cavitation region by doping the oil with a fluorescent dye and using an ultraviolet light source. A paraffinic oil was used as the test fluid; it had the properties shown in Table 1.

RESULTS AND DISCUSSION

Tests were conducted at two different shaft speeds of 1840 and 3000 rpm. At each speed four levels of the supply pressure, p_s , were examined ranging from 13.6 KPa (2 psig) to 54.4 KPa (8 psig) at intervals of 13.6 KPa (2 psi). Visualization of the extent of the cavitation and also of flow details inside the cavitation region was accomplished by adding fluorescent dye to the lubricant and using an ultraviolet light source. The cavitation region was scanned with the pressure transducer to determine the location and the value of the sub-cavity pressure loop immediately upstream of the point where cavitation started. These correspond to the location, θ_0 , and value, p_{min} , of the minimum pressure, respectively, in the full fluid film. The extent of the cavitation region was also determined from the pressure measurements. The results are summarized in Table 2, and discussed in more detail in the following sections.

Flow Visualization

An interesting phenomenon that was typical for all the cases examined is a reverse flow which can be seen at the downstream end of the cavitation. This reverse flow is observed as oil streams on the inner diameter of the transparent bearing flowing slowly backward between the typical oil streamers of the cavitation region. As the front of the backward moving oil reached a certain point upstream of the end of the cavitation region it stopped and the oil was then carried rapidly forward by the moving shaft. The cycle of this backward and forward motion is constantly repeated at a low frequency. Occasional lateral fluctuations of the oil streamers were also observed. This lateral motion originated at the upstream boundary of the cavitation and is probably related to cavity instability [7].

Still pictures of the cavitation region at a shaft speed of 1840 rpm are shown in Figs. 5(a) to (d) for the four levels of supply pressure. The direction of shaft rotation is from bottom to top. The horizontal reference line across each picture marked $\theta = 0$ indicates the angular location of the maximum clearance. Below the reference line the bearing's clearance is diverging while above this line the clearance is converging in the direction of shaft rotation. Figure 5(a), corresponding to $p_s = 13.6$ KPa (2 psig), shows a deep penetration of the cavitation region into the converging portion of the bearing clearance. The downstream end of the cavitation is well rounded and the reverse flow, clearly seen as the gray area, covers a relatively large portion of the downstream boundary of the cavity. As the supply pressure is increased the downstream end of the cavitation retreats toward the maximum clearance line. The size of the reverse flow region is reduced and the downstream end of the cavity becomes more pointed. At

$p_s = 27.2$ KPa the cavitation still penetrates into the converging portion of the bearing's clearance (Fig. 5(b)). A further increase in the supply pressure, to $p_s \geq 40.8$ KPa, causes the termination of the cavitation at or upstream of the maximum clearance line (Figs. 5(c) and (d)).

There is some disagreement in the literature of cavitation as to whether the oil is carried over the cavitation region entirely by the oil streamer or partially by the streamers and partially between the cavity and the moving shaft. The somewhat gray background between the streamers in all four cases shown in Figs. 5(a) to (d) suggests that the oil is not carried over entirely by the streamers, but also between the cavity and the moving shaft.

Pressure Measurement

Pressure traces of the cavitation regions corresponding to the four cases shown in Figs. 5(a) to (d) are presented in Figs. 6(a) to (d). The axial pressure distribution at various circumferential positions is presented in a dimensionless form as the measured pressure, p , normalized by the supply pressure, p_s . In each case the pressure distribution is shown at the point of minimum pressure ($\theta = \theta_0$), at the start of the cavitation region ($\theta = \theta_{st}$), and at the end of the cavitation region ($\theta = \theta_{end}$). Also at least one trace is shown in the full fluid film outside the downstream end of the cavitation. The slight asymmetry of the pressure profiles about the center-line of the bearing, $Z/L = 0$, is probably due to the lack of perfect alignment of the bearing and shaft. Such misalignment could result from the hydrodynamic load acting on the cantilevered housing.

As can be seen from Table 2 and Figs. 6(a) to (d) the minimum film pressure at 1840 rpm is -13.6 KPa (-2 psig) regardless of the supply pressure p_s . The location θ_0 of the minimum pressure is affected by

p_s , ranging from $\theta_0 = 190^\circ$ at $p_s = 13.6$ KPa to $\theta_0 = 205^\circ$ at $p_s = 54.4$ KPa. At the start of the cavitation, $\theta = \theta_{st}$, there is a sharp drop in the pressure at both ends of the bearing ($Z/L = \pm 0.5$) from the supply pressure ($p/p_s = 1$) to a value slightly above the atmospheric pressure ($p/p_s = 0$). Cavitation starts about 5 to 10 degrees downstream of the minimum pressure location. The pressure in the cavitation region remains fairly constant over a large portion of the circumferential extent of the cavity. However, in the last 45° of circumferential extent of the cavitation, the pressure gradually rises until it smoothly joins the full film pressure outside the downstream end of the cavitation.

From Figs. 6(a) to (d) it is clear that the pressure in the cavitation region is not constant. As a matter of fact relatively high pressures exist in the cavitation region where the cavitation penetrates deeply into the converging portion of the bearing clearance, as shown in Figs. 6(a) and (b). In these cases the pressure inside the cavitation region reaches values that are even above the supply pressure that is $p/p_s > 1$. In Figs. 6(c) and (d), where the cavitation penetrates only slightly into the converging clearance or is confined entirely to the diverging clearance, the cavitation pressure is below the supply pressure, $p/p_s < 1$, throughout the cavitation region. Even in these cases, however, the variation in the cavity pressure is significant.

The pressure fluctuations shown in Fig. 6(a) near the downstream end of the cavitation are the result of unsteadiness in the pattern of the oil streamers. The lateral motion of the oil streamers is more pronounced in the case of low supply pressure, p_s . As was mentioned above this instability originates at the start of the cavitation but its effect on the pressure is felt mostly toward the end of the cavitation where the pressure level is much higher.

The pressure traces at shaft speed of 3000 rpm are presented in Figs. 7(a) to (d) for the four levels of supply pressure as before. The most noticeable difference between the 3000 and 1840 rpm cases is the lower value of the minimum pressure at the higher speed case. By increasing the shaft speed from 1840 to 3000 rpm the minimum pressure dropped from -13.6 KPa (-2 psig) to -27.2 KPa (-4 psig) and, in one case when $P_s = 13.6$ KPa, to -34 KPa (-5 psig). The angular location of the minimum pressure, θ_0 , is about 3° to 7° further downstream compared to the 1840 rpm case. The cavitation extent is also somewhat larger because of the greater hydrodynamic effect at the higher speed, and the end of the cavitation region at 3000 rpm is located a few degrees downstream of the corresponding end at 1840 rpm. The pressure inside the cavity behaves similar to the lower speed case. It remains fairly constant over a large portion of the cavity but in the last 45° to 50° of the circumferential extent the pressure starts to rise gradually to the value of the full film pressure outside the downstream end of the cavitation.

Cavitation Region Content

In order to check the gas content of the cavity, the pressure transducer was taken off. A sample tube originally under a hard vacuum was attached to the pressure tap hole, and the cavity content was sucked into the sample tube. The content of the sample tube was then analyzed by means of a mass spectrometer and was found to contain air. No oil vapors were found to be present in the cavitation region. This quick check, which by no means is meant to be conclusive, may suggest that the mechanism of the cavitation was a release of dissolved air as the oil pressure fell below the saturation pressure.

CONCLUDING REMARKS

Visual observations and pressure measurements in the cavitation zone of a submerged journal bearing were performed. Tests were ran at speeds of 1840 and 3000 rpm. At each speed four different levels of the ambient supply pressure were applied ranging from 13.6 KPa (2 psig) to 54.4 KPa (8 psig). Addition of a fluorescent dye to the oil and use of an ultra violet light source enabled close examination of flow details inside the cavitation region. A strong reverse flow was detected inside the cavitation area adjacent to its downstream end.

Pressure field mapping of the cavitation region was accomplished by a scanning pressure transducer. Significant pressure variations were found inside the cavitation region at the downstream portion of its circumferential extent. These pressure variations were present in all the cases tested regardless of speed and ambient supply pressure. In cases where the cavitation penetrates into the converging clearance portion of the bearing, pressures inside the cavitation region exceeded the ambient pressure.

Theoretical cavitation models in present use are based on the assumption of a constant cavitation pressure. From the experimental results presented in this paper it seems that this assumption is incorrect in the case of enclosed cavitations.

It is postulated that oil which is saturated with air under atmospheric pressure becomes over-saturated in the sub-cavity pressure loop. This acts as a source of air which is subsequently pressurized by the viscous drag induced by rotor motion, and this increase in pressure forces the air back into solution at the other end of the cavity. This continuing process of air coming out and going back into solution is a possible mechanism that

controls the pressure variation in the cavity. Further experimental and theoretical work is needed to more fully explore the effect of air solubility.

As discussed in the text the misalignment associated with the cavitation mounting of the housing could induce asymmetric pressure profiles. Also the method of locating the point of maximum clearance is subject to a possible error of $\pm 5^\circ$. However, these two experimental deficiencies do not affect the basic conclusion that the pressure inside the cavitation region is not constant.

ACKNOWLEDGEMENT

The research reported in this paper was performed while the first author held a NRC-NASA research associateship at NASA Lewis Research Center, Cleveland, Ohio.

REFERENCES

1. Dowson, D. and Taylor, C. M., "Fundamental Aspects of Cavitation in Bearings," Cavitation and Related Phenomena in Lubrication, Proc. of the 1st Leeds-Lyon Symposium on Tribology, Mechanical Engineering Publ., Ltd., New York, 1974, pp. 15-26.
2. Floberg, L., "Cavitation Boundary Conditions with Regard to the Number of Streamers and Tensile Strength of the Liquid," Cavitation and Related Phenomena in Lubrication, Proc. of the 1st Leeds-Lyon Symposium on Tribology, Mechanical Engineering Publ., Ltd., New York, 1974, pp. 31-35.
2. Findlay, J., "Cavitation in Mechanical Face Seals," ASME Journal of Lubrication Technology, Vol. 90, No. 2, Apr. 1968, pp. 356-364.
4. Nau, B. S., "Observation and Analysis of Mechanical Seal Film Characteristics," ASME Journal of Lubrication Technology, Vol. 102, No. 3, July 1980, pp. 341-349.

5. Pan, C. H. T., "An Improved Short Bearing Analysis for the Submerged Operation of Plain Journal Bearings and Squeeze-Film Dampers," ASME Journal of Lubrication Technology, Vol. 102, No. 3, July 1980, pp. 320-332.
6. Pan, C. H. T., and Ibrahim, R. A., "Cavitation in a Short Bearing with Pressurized Lubricant Supply," ASME Paper No. 80-C2-Lub-67 to be presented at the SME-ASLE International Lubrication Conf., San Francisco, Aug. 18-21, 1980.
7. Savage, M. D. C., "Cavity Instability," Cavitation and Related Phenomena in Lubrication, Proc. of the 1st Leeds-Lyon Symposium on Tribology, Mechanical Engineering Publ., Ltd., New York, 1974, pp. 53-54.

TABLE 1. - LUBRICANT PROPERTIES

Temperature, T, °C	-29	-18	38	99	149	204
Viscosity, N sec/m ²	2.1	0.84	0.026	0.0047	-----	0.0017
Vapor pressure, mmHg (absolute)	---	----	0.1	-----	5.3	9.2
Specific gravity = 0.8285						

TABLE 2. - RESULTS OF MINIMUM FILM PRESSURE AND CAVITATION EXTENT

Shaft speed, N, rpm	Supply pressure, P _s KPa	Minimum pressure location, θ ₀ , deg	Minimum film pressure, P _{min} , KPa	Cavitation start, θ _{st} , deg	Cavitation end, θ _{end} , deg
1840	13.6	190	-13.6	200	75
	27.2	197	↓	210	40
	40.8	200		210	15
	54.4	205		210	355
3000	13.6	193	-34.0	200	75
	27.2	200	-27.2	210	45
	40.8	207	-27.2	215	20
	54.4	210	-27.2	220	5

ORIGINAL PAGE IS
OF POOR QUALITY

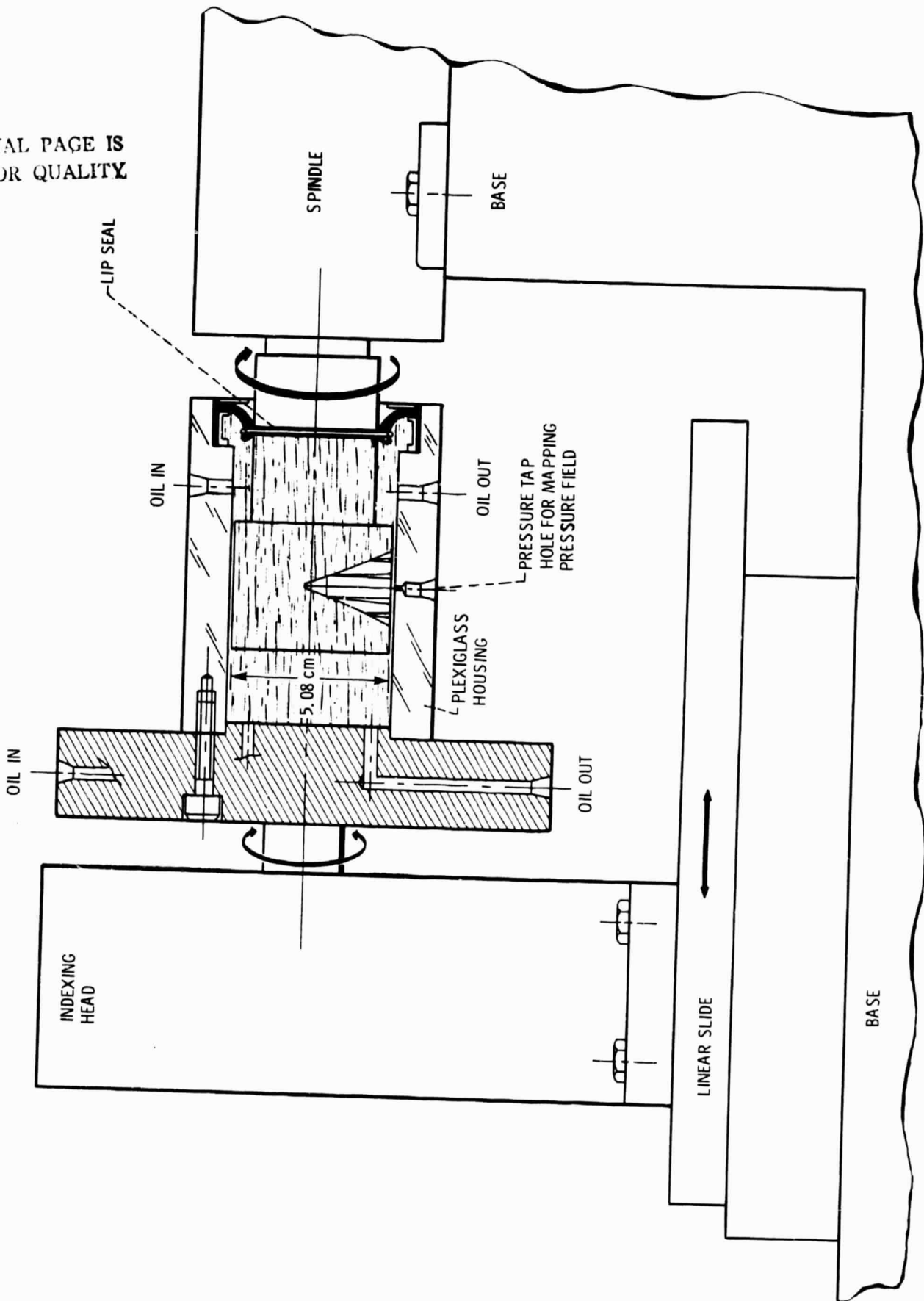


Figure 1. - Schematic of test rig.

ORIGINAL PAGE IS
OF POOR QUALITY

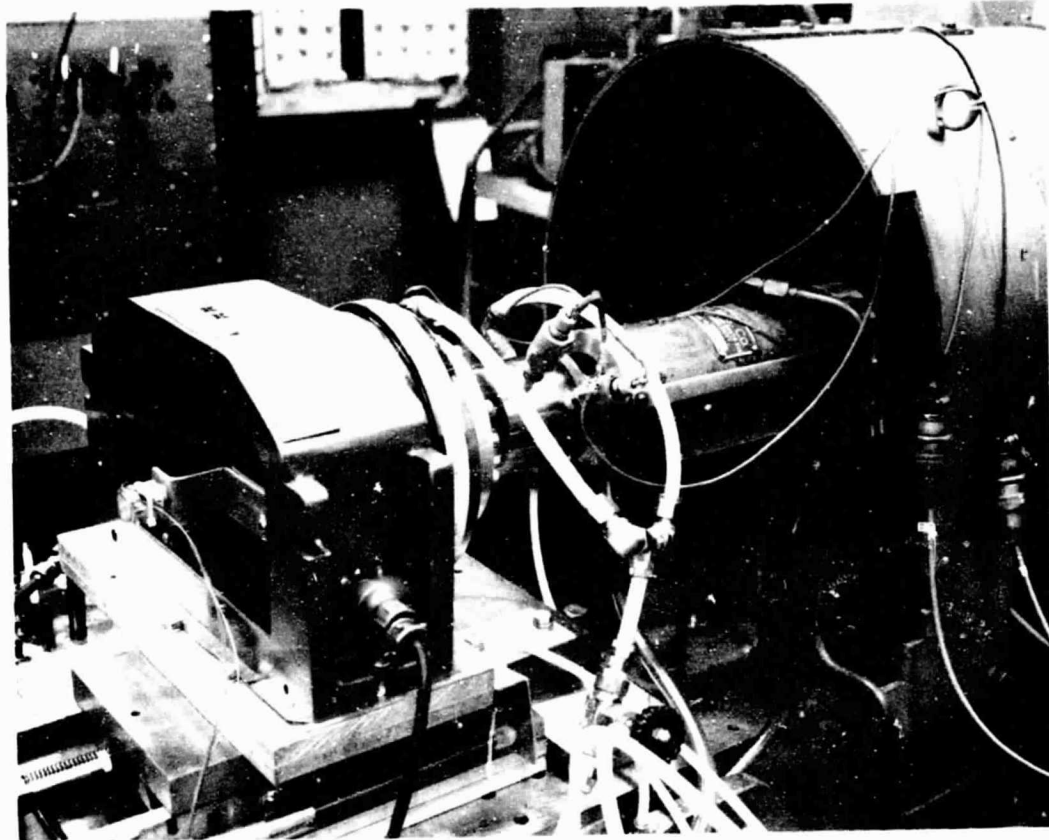


Figure 2. - Test apparatus.

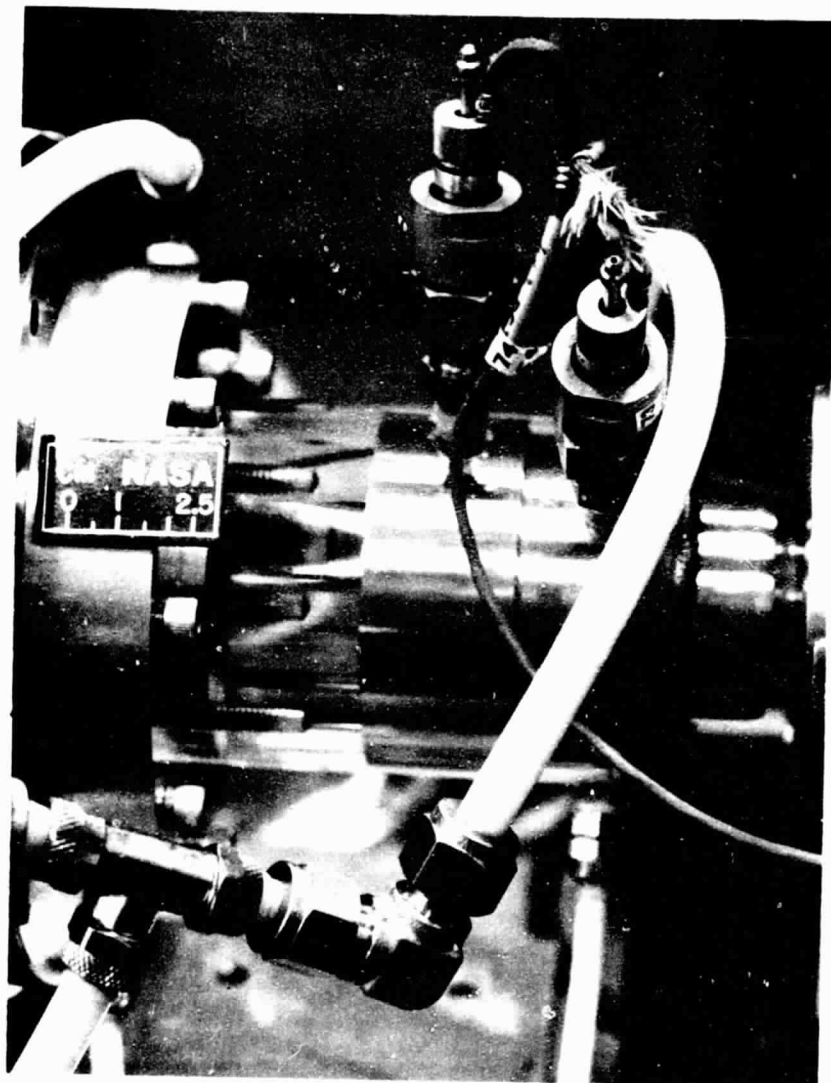


Figure 3. - Test bearing.

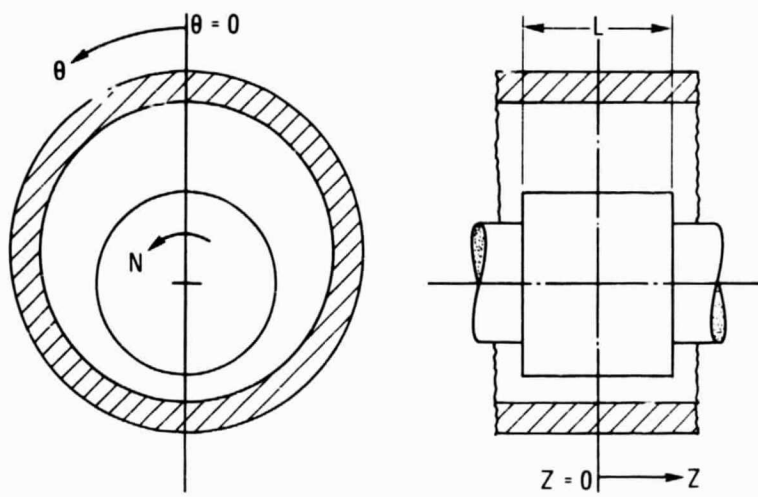
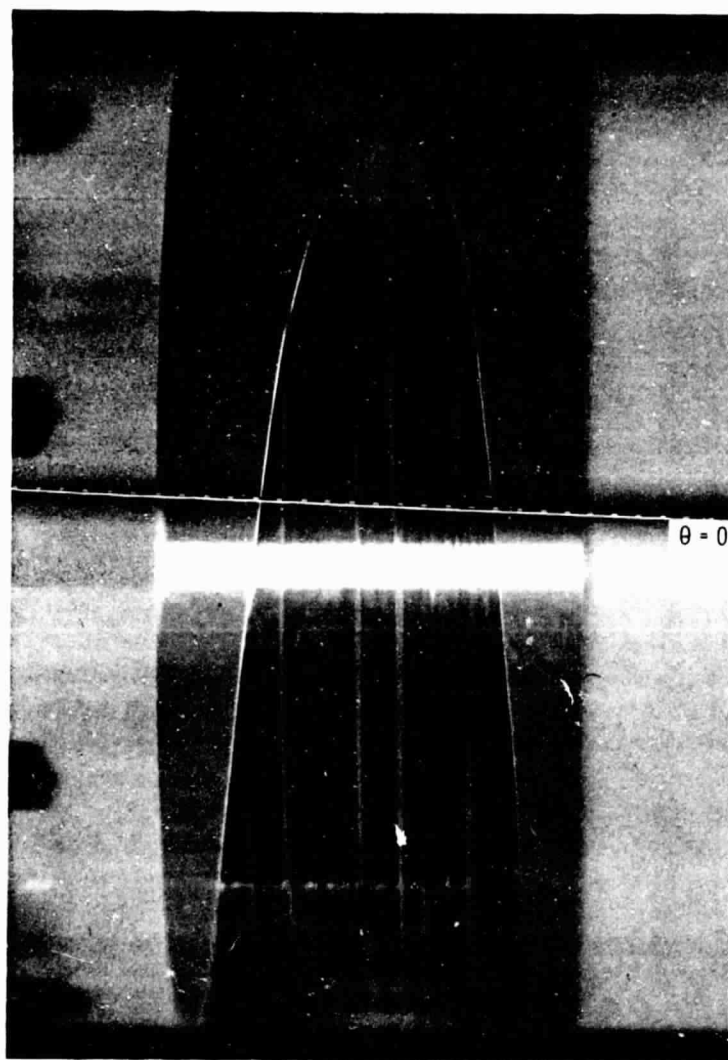


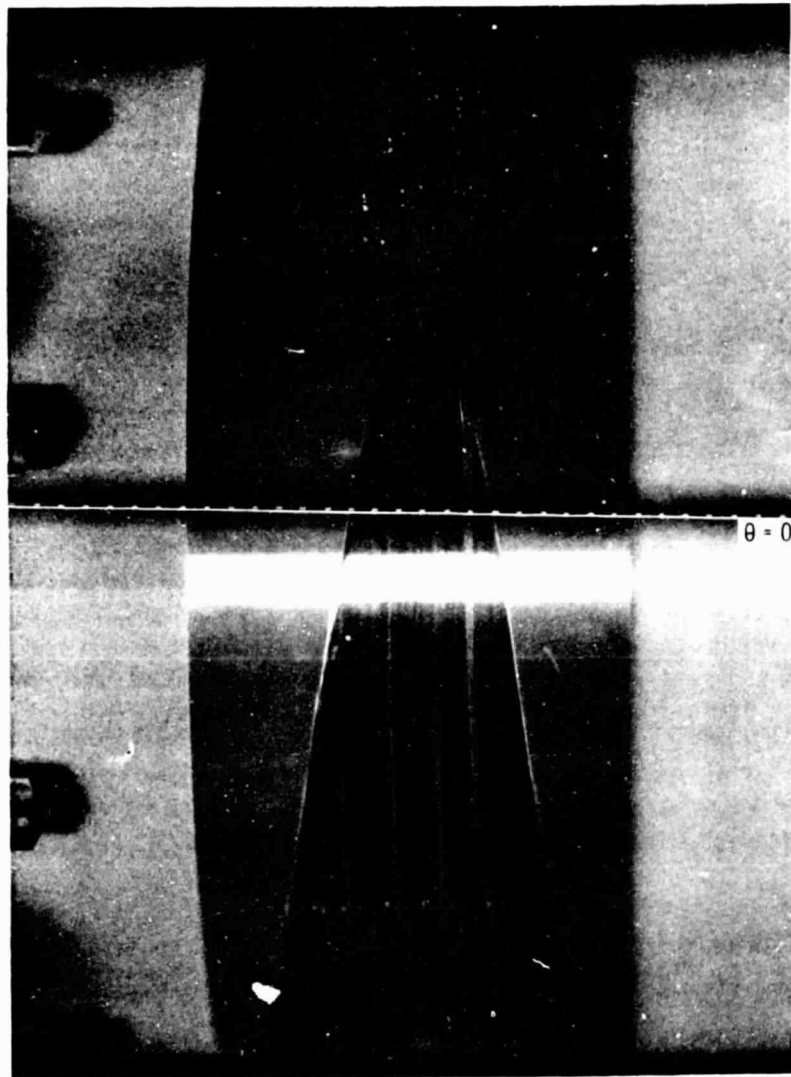
Figure 4. - Schematic of bearing showing reference planes for the angular and axial positions of pressure measurements.

ORIGINAL PAGE IS
OF POOR QUALITY



(a) $N = 1840$ rpm; $p_s = 13.6$ KPa.

Figure 5. - Cavitation zone.



(b) $N = 1840$ rpm; $p_s = 27.2$ KPa.

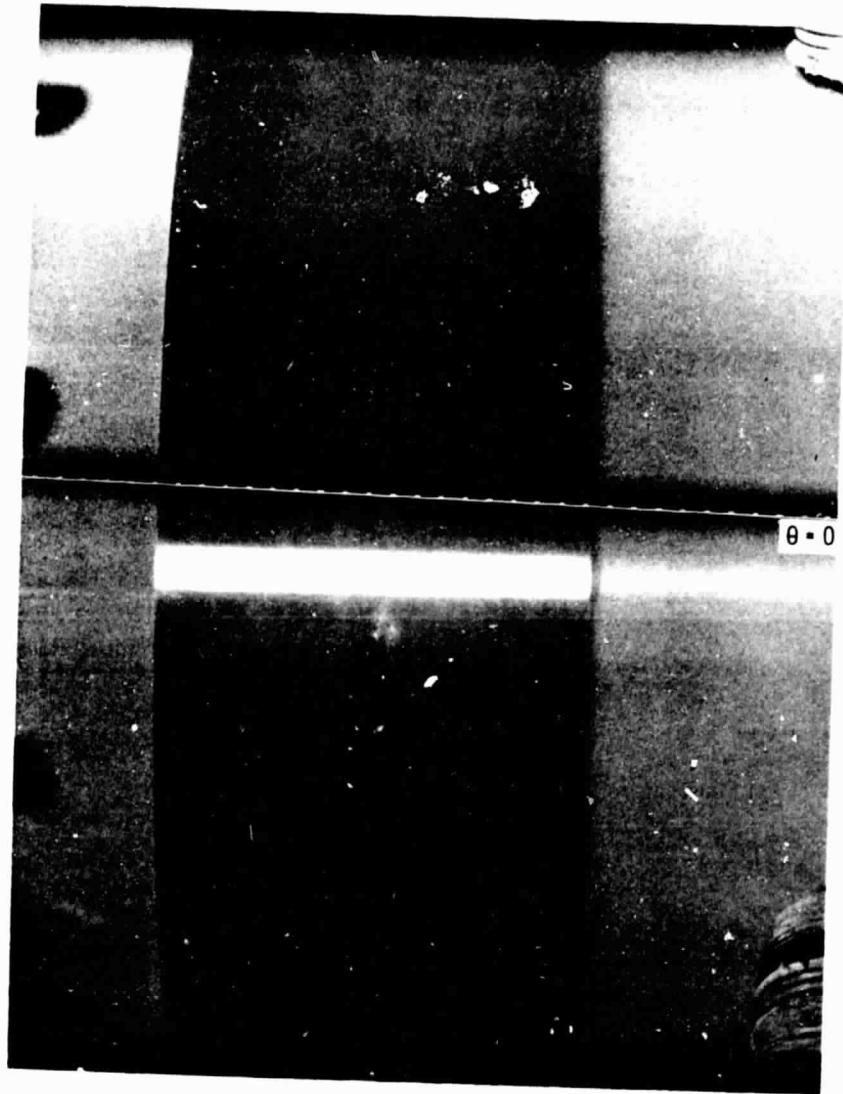
Figure 5. - Continued.

ORIGINAL PAGE IS
OF POOR QUALITY



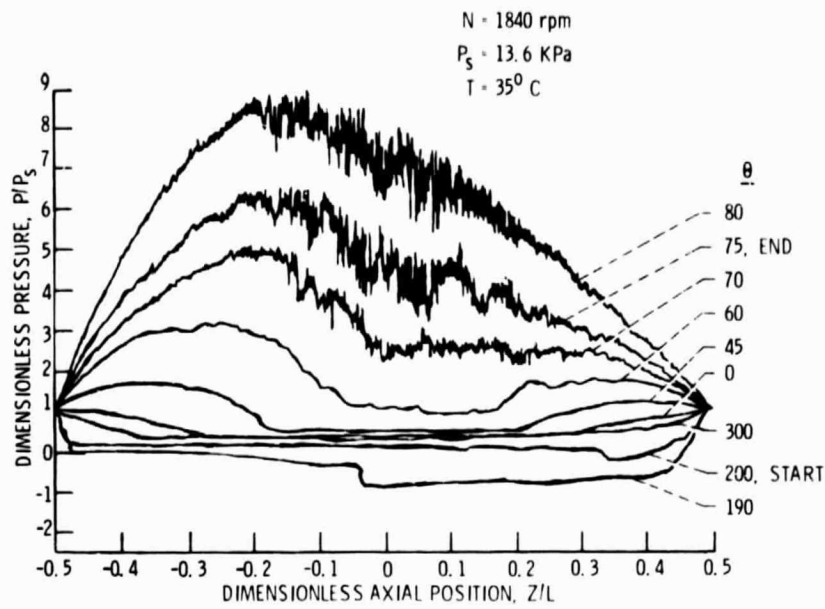
(c) $N = 1840$ rpm; $p_s = 40,8$ KPa.

Figure 5. - Continued.

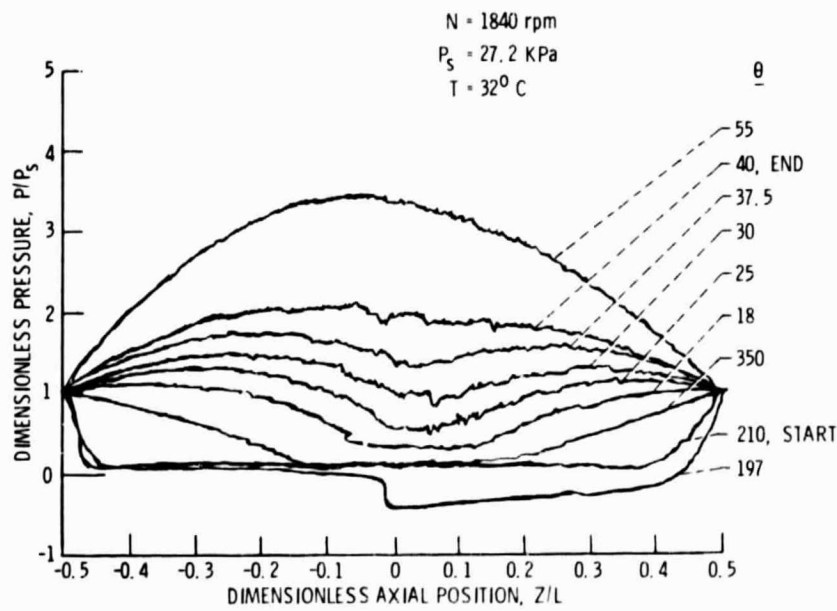


(d) $N = 1840$ rpm; $p_s = 54.4$ KPa.

Figure 5. - Concluded.

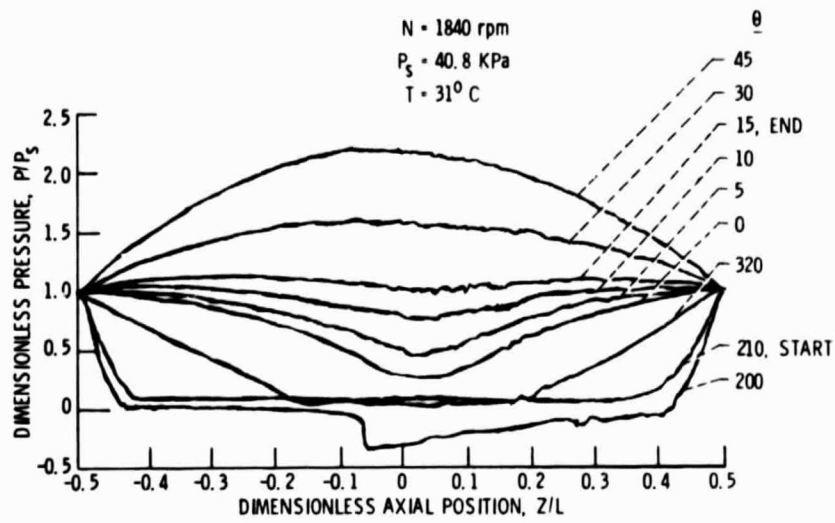


(a) $N = 1840 \text{ rpm}$; $P_s = 13.6 \text{ KPa}$.

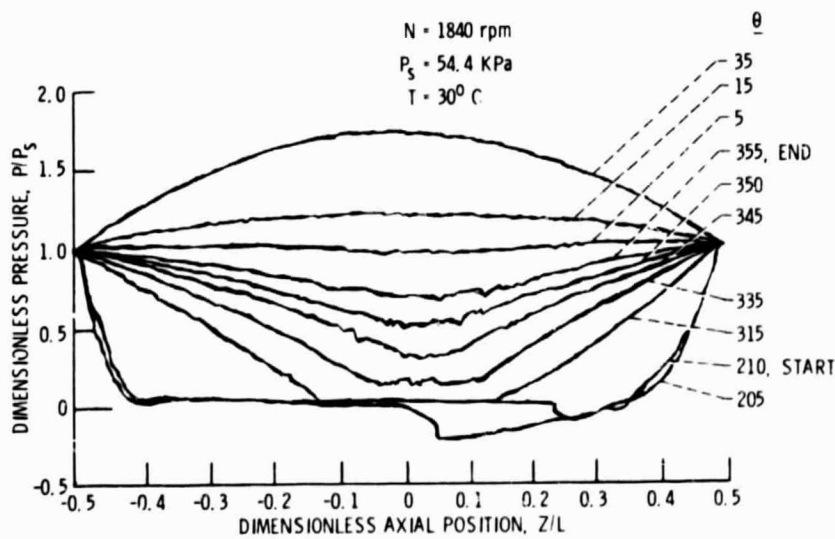


(b) $N = 1840 \text{ rpm}$; $P_s = 27.2 \text{ KPa}$.

Figure 6 - Cavitation zone pressure map.



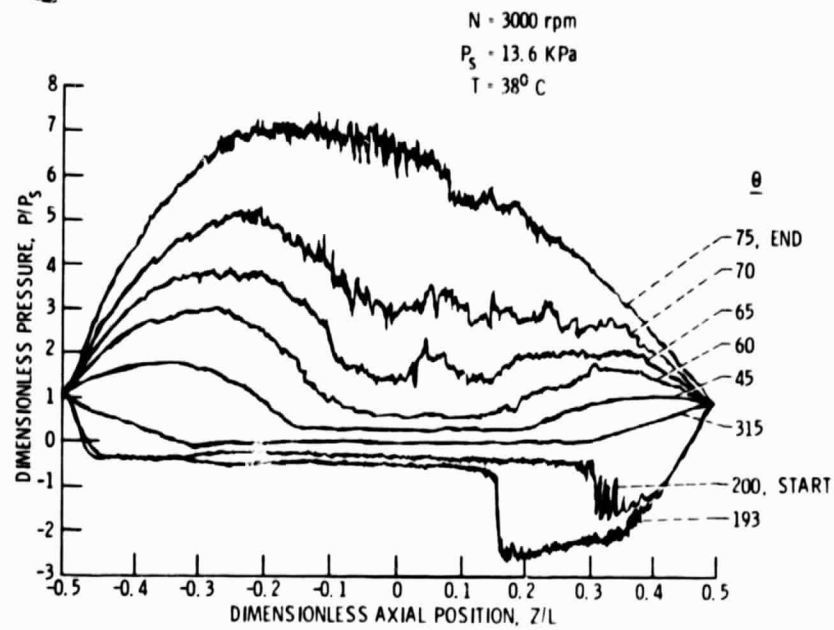
(c) $N = 1840 \text{ rpm}$; $P_s = 40.8 \text{ KPa}$.



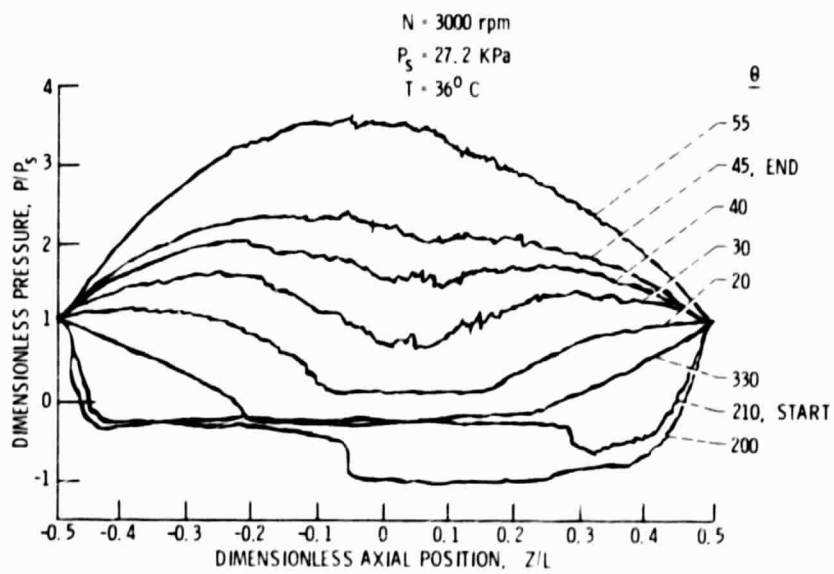
(d) $N = 1840 \text{ rpm}$; $P_s = 54.4 \text{ KPa}$.

Figure 6. - Concluded.

ORIGINAL PAGE IS
OF POOR QUALITY



(a) $N = 3000 \text{ rpm}$; $P_s = 13.6 \text{ KPa}$.



(b) $N = 3000 \text{ rpm}$; $P_s = 27.2 \text{ KPa}$.

Figure 7. - Cavitation zone pressure map.

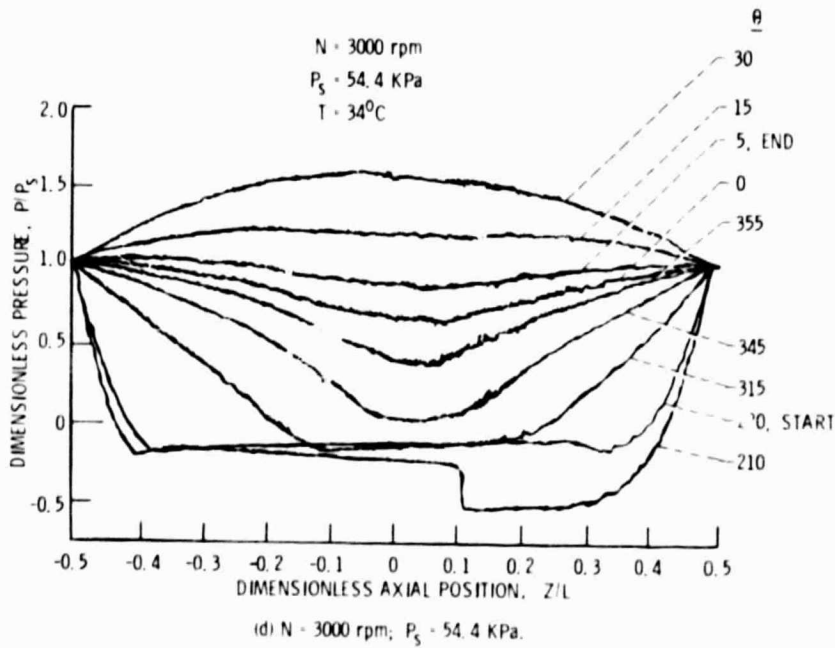
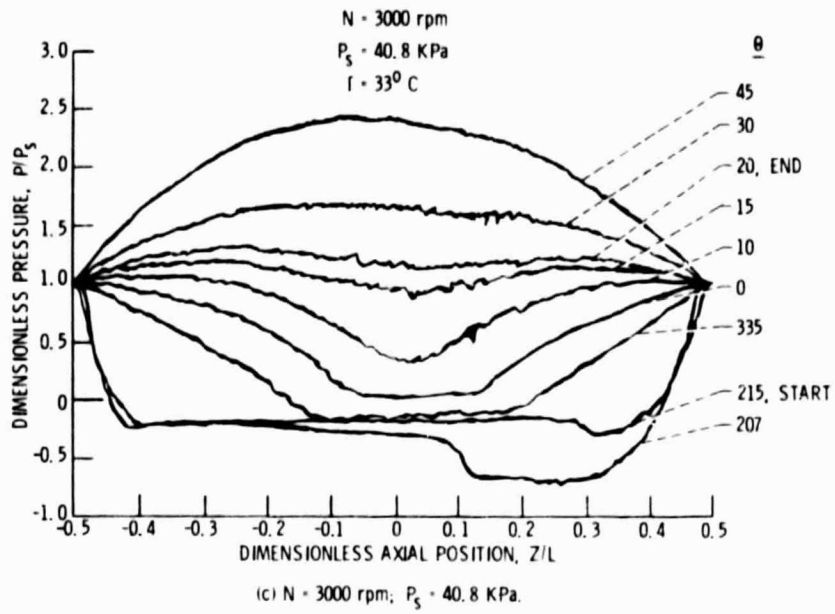


Figure 7. - Concluded.

1 Report No NASA TM-81582	2 Government Accession No	3 Recipient's Catalog No	
4 Title and Subtitle OBSERVATION OF PRESSURE VARIATION IN THE CAVITATION REGION OF SUBMERGED JOURNAL BEARINGS		5 Report Date	
		6 Performing Organization Code	
7 Author(s) I. Etsion and L. P. Ludwig		8 Performing Organization Report No E-555	
		10 Work Unit No	
9 Performing Organization Name and Address National Aeronautics and Space Administration Lewis Research Center Cleveland, Ohio 44135		11 Contract or Grant No	
		13 Type of Report and Period Covered Technical Memorandum	
12 Sponsoring Agency Name and Address National Aeronautics and Space Administration Washington, D.C. 20546		14 Sponsoring Agency Code	
		15 Supplementary Notes Prepared for the Lubrication Conference sponsored by the American Society of Mechanical Engineers, New Orleans, Louisiana, October 11-14, 1981.	
16 Abstract Visual observations and pressure measurements in the cavitation zone of a submerged journal bearing are described. Tests were performed at various shaft speeds and ambient pressure levels. Some photographs of the cavitation region are presented showing strong reverse flow at the downstream end of the region. Pressure profiles are presented showing significant pressure variations inside the cavitation zone, contrary to common assumptions of constant cavitation pressure.			
17 Key Words (Suggested by Author(s)) Journal bearings Cavitation in bearings		18 Distribution Statement Unclassified - unlimited STAR Category 37	
19 Security Classif (of this report) Unclassified	20 Security Classif (of this page) Unclassified	21 No. of Pages	22 Price*